Structural Characterization of Methylsilsesquioxane-Based Porous Low-k Thin Films Using X-ray Porosimetry

Hae-Jeong Lee, Christopher L. Soles, Da-Wei Liu, Barry J. Bauer, Eric K. Lin, and Wen-li Wu

Polymers Division, National Institute of Standards and Technology, Gaithersburg, MD, 20899

Abstract

Methylsilsesquioxane based porous low-k dielectric films with different porogen loading have been characterized using X-ray porosimetry to determine their pore size distribution, average density, wall density and porosity. By varying the porogen content from 1 % to 30 %, the porosity and the average pore size changed from 12 % to 34 % and from 10 Å to 15 Å in radius, respectively. The wall density was found to be independent of the porogen content and it appeared that the porogen is not 100% effective in generating pores. Pore size of these samples was also obtained from small angle neutron scattering measurements and the results were found to be consistent with that from XRP.

Introduction

Highly porous materials are the primary candidates for low dielectric constant (low-k) interlevel dielectrics in future integrated circuit (IC) chips. However, depending on structure details, porosity can also adversely affect other properties crucial to chip performance such as mechanical strength, electrical properties and Cu metal diffusion. Therefore, it is important to characterize the on-wafer structure of these porous thin films in order to optimize the processing conditions and the resulting physical properties. Recently several promising methodologies were developed including focused positron beam techniques (1), ellipsometry porosimetry (EP) (2), and a combination of specular X-ray reflectivity (SXR), small angle neutron scattering (SANS) and ion-beam scattering (3). However, there are limitations inherent to each of these methodologies. The SANS technique suffers from the limited availability of neutron scattering facilities. The positron beam technique is primarily limited to small pores less than 20 Å in diameter and further requires a high vacuum environment. EP assumes that optical polarizability of adsorbate and adsorbent are additive, this assumption is not immediately evident.

Recently, we have developed an X-ray porosimetry (XRP) technique for characterizing porous low-k thin films (4). XRP is analogous to traditional adsorption/desorption techniques in which the amount of gaseous probe molecules (in this work, toluene) condensed inside the porous sample was measured as a function of partial pressure. In XRP the toluene uptake is directly determined from the critical angle for total X-ray reflection, no assumption is needed. In addition, the change in film thickness upon adsorption/desorption can be determined precisely. The Kelvin equation is used as an approximate relationship between the pore size and partial pressure to calculate the pore size distribution (PSD). This provides a simple but powerful tool to determine PSD within a porous thin film. We illustrate the power of this new methodology by reporting structural information including porosity, PSD, average film density, and matrix material density of methylsilsesquioxane (MSQ) based porous low-k thin films. A definite correlation between the porogen loading and the pore structure was observed.

Experimental

Porous thin films were prepared through templated vitrification of low molecular mass siloxane oligomers using macromolecular cross-linked porogen particles (5). Porosity was controlled by varying porogen loading from 1 % to 30 % by mass. The elemental composition of the films was determined from ion beam scattering, through a combination of Rutherford backscattering, grazing angle incident scattering and forward recoil scattering. SXR experiments were performed at grazing incident angles on a modified θ–2θ X-ray diffractometer to monitor changes in the electron density during the adsorption/desorption of toluene molecules in the porous thin film. The X-ray source was finely focused copper K_α radiation with a wavelength, λ, of 1.54 Å. First, the samples were conditioned in the reflectometer at 175 °C in vacuum for 2 h before cooled down to 20 °C. After collecting the reflectivity, a stream of toluene saturated air was passed over the samples. This air was saturated with toluene by slowly bubbling through liquid toluene at (20 ± 0.1) °C (6). The sample temperature, from 20 °C to 125 °C, was used to control toluene partial pressure. After each temperature change, 30 min. was allowed for thermal equilibration before the ensuing reflectivity measurements were performed.

The results from XRP were compared with those from the combination of SANS/SXR technique described elsewhere (3). The SANS measurements were performed on the NG1 beam line at the National Institute of Standards and Technology Center for Neutron Research. The neutron wavelength was 6 Å with a wavelength spread (FWHM) $\Delta\lambda/\lambda$ of 0.14.

Results and Discussion

Fig. 1 shows experimental SXR curves for films of varying porogen content both under vacuum and in the saturated toluene atmosphere. The reflectivity data is presented as the logarithm of the reflected intensity

($I_{reflected}/I_{incident}$; I is beam intensity) as a function of q ($q = (4\pi/\lambda)\sin\theta$; θ is the grazing incident angle of the X-ray beam). As the incident angle increases, the X-rays begin to penetrate the film at a critical value of q, beyond which point the reflected intensity drops sharply. This critical angle, in units of q_c^2 ($Å^{-2}$), is used to calculate the average mass density of the film. In Fig. 1 it is clear that the density of porous thin film decreases as increases in porogen contents. The elemental composition and the densities of the films are summarized in Table I.

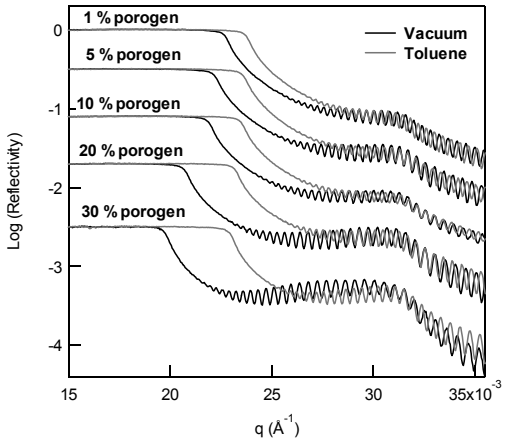

Fig. 1 SXR curves of the MSQ based low-k thin films with varying porogen loading. The black and gray curves indicate the experimental data taken under vacuum and in the saturated toluene atmosphere, respectively.

Table I. Structural properties of MSQ based porous low-k thin films with varying porogen loading contents.

Progen loading contents	Atomic composition (Si: O: C: H, %)	q_c^2 (E-4) ($Å^{-2}$)	Average density (g/cm^3)	Wall density (g/cm^3)	Porosity (%)
1 %	20: 24: 16: 40	5.21	1.18	1.34	12
5 %	18: 23: 15: 44	4.98	1.12	1.34	16
10 %	17: 22: 15: 46	4.86	1.09	1.33	18
20 %	17: 21: 13: 49	4.35	0.97	1.34	27
30 %	19: 25: 15: 41	3.95	0.89	1.35	34

The relative standard uncertainties of the atomic composition, q_c^2, density, and porosity are ± 5 %, 0.05 $Å^{-2}$, 0.05 g/cm^3, and 1 %, respectively.

Fig. 1 also shows that the critical angle of the porous film moves to higher q in the presence of the saturated toluene vapor. This is resulted from the capillary condensation of toluene inside the pores accessible to the solvent vapor, such as pores interconnected to the free surface. The average mass density of the film is related to the porosity and matrix density of the film through the following relations given in eq. (1) and (2).

$$\rho_{ave} = \rho_w \times (1–P) \quad (1)$$

$$\rho_{ave,\ toluene} = \rho_w \times (1–P) + \rho_{toluene} \times P \quad (2)$$

where ρ_w, P, $\rho_{ave,\ toluene}$, and $\rho_{toluene}$ are the density of the wall material between the pores, the porosity of the film, average mass density of porous thin film saturated under toluene vapor and average mass density of toluene solvent (0.865 g/cm^3) respectively.

By comparing the vacuum and the toluene saturated data, one can calculate the amount of toluene adsorbed, and hence the total pore volume. With two unknowns and two equations, wall material density and porosity can be determined. The wall density calculated by this method is an average of the wall material and any unfilled pores such as closed pores or pores smaller than the toluene molecules. The porosity of the films increases from 12 % to 34 % and wall density stays unchanged as the porogen loading increases. Interestingly, porosity of the film with 1 % porogen content is 12 %, indicating the porous nature of the starting MSQ material. Surprisingly though, total porosity is only 34 % at a porogen loading of 30 %, suggesting that the porogen used is not 100% effective generating pores. The porosity and wall density results from these films are summarized in Table I.

Fig. 2 displays a series of reflectivity curves as a function of the toluene partial pressure for the 30 % by mass porogen film. It is evident that the critical angle shifts to lower values as the sample temperature was raised – equivalent to a decrease in toluene partial pressure. Notice that most of the desorptions occurred in the partial pressure range from 0.2 to 0.3. This indicates a large population of pores being drained at these intermediate pressures. To analyze these adsoption/desorption data, we use the Kelvin equation to estimate the pore size r_c. In this expression γ is the liquid surface tension, V_m is the molar volume of the liquid, P is the partial pressure, and P_0 is the equilibrium pressure at temperature T.

$$r_c = \frac{2V_m\gamma}{-RT}\frac{1}{\ln(P/P_o)} \quad (3)$$

The toluene uptakes calculated from the critical angle results are plotted as a function of the partial pressure in Fig. 3. In the case of the film with 1 % porogen content, the uptake saturates at low partial pressures and the adsorption and desorption branches coincide. This is characteristic of micropore filling and is also consistent with the notion that MSQ matrix materials are microporous. An adsorption/desorption hysteresis loop, indicative of the presence of mesopores, become evident as the porogen content increases. Note that the adsorption branch is always broader than the desorption branch. This does not necessarily suggest a more narrow pore size distribution of desorption branch, rather reflects the fact that desorption must proceed through smaller pores that block the desorption of the larger pores (i.e., the ink bottle effect). Such pore blocking on the desorption branch of the hysteresis loop is well documented in the porosimetry literature (7). In an ink bottle-shape pore, capillary condensation on the adsorption branch would be dominated by the radius of curvature of the larger pore whereas

desorption is governed by the radius of the narrow neck. This results in a simultaneous draining of both the small and large mesopores, and hence a sharp drop in the desorption curve, as seen in Fig. 3.

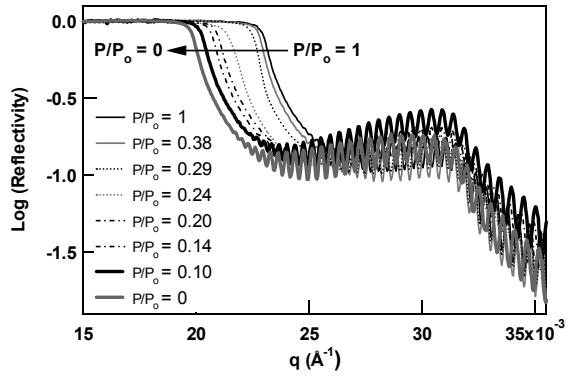

Fig. 2 SXR curves as decreases in the toluene partial pressure for a porous MSQ low-k dielectric films. The standard uncertainty in Log (Reflectivity) is less than the line width.

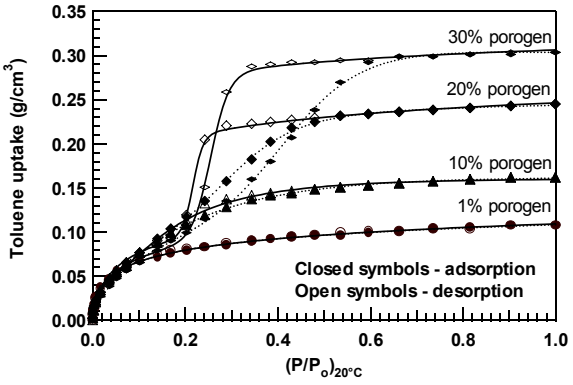

Fig. 3 Adsorption/desorption isotherms for a series of porous MSQ films formulated with varying loading of porogen. The lines are smooth fits using the sum of a sigmoidal and a lognormal function.

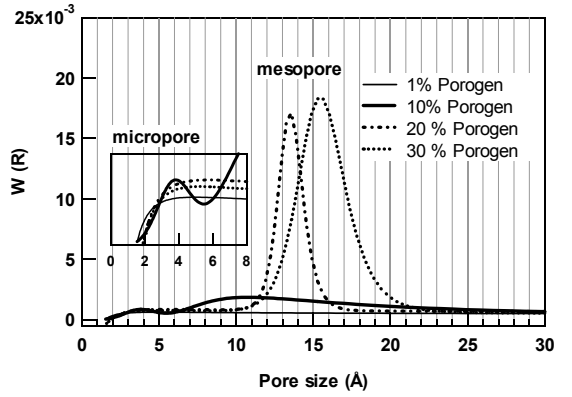

Fig. 4 Pore size distributions from the fits in Fig. 3 of porous MSQ thin films with varying porogen loading contents.

The partial pressure in Fig. 3 can be converted into the pore size through eq. (3) thereby establishing a PSD (Fig. 4). According to porosimetry tradition we use the desorption branch for PSD analysis. As the porogen loading increases, the pore size at maximum population increases from 10 Å to 15 Å in radius. Note that we can also distinguish the inherent micropores of the matrix from porogen-created mesopores. These results clearly demonstrate the prowess of XRP as a methodology for the determining detailed structural information of porous low-k films.

We have also performed SANS measurements to measure pore sizes and to compare to the XRP PSDs. Fig. 5 displays the SANS data which can easily be fit using a Debye model to extract an average pore size. For the film with 30 % porogen the fit gives an average pores size of approximately 10 Å in radius, which is comparable to the 15 Å to 16 Å obtained by XRP.

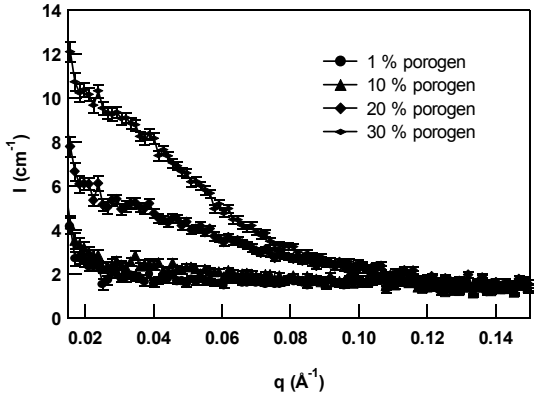

Fig. 5 SANS data of porous MSQ thin films with varying porogen contents.

Conclusion

We have applied X-ray porosimetry to determine structural properties of MSQ based porous thin films with different porogen loading. The average film density, matrix material density, porosity, and PSD were determined, and the pore size results were similar to those from SANS measurements. This work demonstrates the applicability of XRP to characterize porous thin films.

References

(1) D. W. Gidley, W. E. Freize, T. L. Dull, J. Sun, A. F. Yee, C. V. Nguyen, D. Y. Yoon, *Appl. Phys. Lett*. **76** 1282 (2000).

(2) M. R. Baklanov, K. P. Mogilnikov, V. G. Polovinkin, F. N. Dultsev, *J. Vac. Sci. Technol. B* **18**, 1385 (2000).

(3) W. L. Wu, W. E. Wallace, E. K. Lin, G. W. Lynn, C. J. Glinka, E. T. Ryan, H. M. Ho, *J. Appl. Phys*. **87**, 1193 (2000).

(4) H. J. Lee, C. L. Soles, W. W. Liu, B. J. Bauer, W. L. Wu, *J. Polym. Sci.: Part B: Polym. Phys*. **40**, 2170 (2002).

(5) M. Gallagher, N. Pugliano, M. Roche, J. Calvert, Y. You, R. Gore, N. Annan, M. Talley, S. Ibbitson, A. Lamola, *MRS Spring Meeting*, San Francisco (2001).

(6) The data throughout the manuscript and in the figures are presented along with the standard uncertainty (±) involved in the measurement.

(7) E. O. Kraemer, *A Treatise on Physical Chemistry*, H. S. Taylor Ed., Macmillan, New York, p1661 (1931).